1992

Gibbs Free-Energy Changes for the Growth of Argon Clusters Absorbed on Graphite

Mary Ann Strozak

Gustavo E. Lopez

See next page for additional authors

Citation/Publisher Attribution

Strozak, M.A., Lopez, G. E., & Freeman, D. L. (1992). Gibbs Free Energy Changes for the Growth of Argon Clusters Adsorbed on Graphite. *Journal of Chemical Physics. 97*(6), 4445-4452. doi: 10.1063/1.463887
Available at: http://dx.doi.org/10.1063/1.463887

Gibbs free-energy changes for the growth of argon clusters adsorbed on graphite

Mary Ann Strozak,[a] Gustavo E. Lopez,[b] and David L. Freeman
Department of Chemistry, University of Rhode Island, Kingston, Rhode Island 02881

(Received 6 May 1992; accepted 10 June 1992)

Changes in Gibbs free energies for the process $Ar_{n-1,(a)} + Ar_{(a)} \rightarrow Ar_{n,(a)}$ are calculated by Monte Carlo simulations for Ar clusters physisorbed on a graphite substrate. Calculations are performed for clusters Ar_2 through Ar_{12} at 10 K. Using a simulated annealing procedure, the minimum-energy configurations at 0 K are obtained. In all cases studied minimal-energy two-dimensional structures are found at a distance above the surface identical to that determined for an argon monomer. Some cluster sizes exhibit isomerization between several low-energy configurations during the simulations. This isomerization leads to sampling difficulties that are significantly reduced by using the *J*-walking method. Minima in the Gibbs free energy are found for cluster sizes 7, 10, and 12. An explanation for the location of the minima in the free-energy function is given in terms of cluster structure and energetics.

I. INTRODUCTION

Because clusters bridge the gap between finite and bulk behavior, the study of molecular aggregates has been an active area of research in chemistry and physics for many years. The unusual properties of clusters make them candidates for important practical applications in such areas as coatings, catalytic processes, and electronics. Clusters also play a key role in the theory of homogeneous nucleation.[1] Understanding how clusters form and grow, therefore, enhances our understanding of how phase transitions proceed, as well as providing information needed for the development of useful new materials.

Since many of the properties of clusters are difficult to study experimentally, clusters have been the subject of numerous investigations using computer simulations. For example, it has been learned computationally that certain sized clusters may have different melting and freezing points. In the melting region these clusters oscillate between configurations characteristic of solidlike and liquidlike systems, implying the two phases exit simultaneously over a definite temperature range.[2] These "coexistence region" phenomena apparently only occur for closed-shell clusters known to have extra thermodynamic stability. The relationship between cluster size, structure, and thermodynamic stability for argon clusters[3] and hydrogen fluoride clusters[4] in the vapor phase has been discussed in the literature. The special cluster sizes having extra thermodynamic stability have often been termed "magic numbers," and may be related to the maxima observed experimentally in the mass distribution of both ionized and neutral clusters.[5,6]

The present work is concerned with physisorbed clusters of argon atoms on a graphite surface. Although most of the previous work on clusters is in the vapor phase, the extension of the investigations to the formation of clusters on surfaces is important. In nucleation phenomena, supersaturated systems preferentially condense at surfaces. Additionally, the formation of clusters on surfaces is a problem of practical interest, because many catalytic materials are composed of clusters. Any such catalyst will require some physical support, and understanding cluster growth and behavior on surfaces is crucial to controlling the synthesis of a given material. In spite of the importance of heterogeneous nucleation, the amount of computational work on such systems has been small.

As indicated previously, the current work is concerned with the condensation of rare gases on graphite surfaces. In contrast to clusters, considerable theoretical and experimental information is available for complete solid and liquid monolayers of rare gases on graphite.[7] The study of rare gases on graphite has been of interest because the migration barriers for adatom diffusion in this system are small. As a consequence of these small migration barriers, it is possible to view rare-gas adsorbates on graphite as nearly ideal two-dimensional films. Furthermore, the interactions between rare-gas adsorbates and between the adsorbates and the substrate have been modeled with well-tested and simple potentials. These potentials are believed to be accurate, making the systems ideal for computational study. A commonly used potential for the rare-gas–graphite system is that introduced by Steele.[8,9] This potential has been successfully used since its introduction in Monte Carlo and molecular-dynamics computer simulations of various rare-gas–graphite systems.

As indicated, in contrast to the large body of work on rare-gas films on graphite, only a few computer simulations of argon clusters on graphite are available. Using the Steele potential, Weissmann and Cohan[10] performed molecular-dynamics simulations to study the formation and melting behavior of argon clusters of sizes 6, 7, 8, and 19. They found no three-dimensional structures for these cluster sizes. Three-dimensional structures were observed for a

[a] Present address: Department of Chemistry, Northwestern University, Evanston, IL 60208.
[b] Present address: Departemento de Ciencias y Tecnologia, Universidad Interamericana, San Juan, PR 00919-1293.

 0021-9606/92/184445-08$006.00

much weaker substrate–adatom interaction, i.e., xenon clusters adsorbed on a neon surface.[10] For the argon–graphite system, Weissmann and Cohan found that 7-atom clusters formed a "closed-shell" minimum-energy configuration of hexagonal geometry. The same type of closed-shell structure was observed for the 19-atom cluster. They also noted that at low temperatures all the clusters exhibited only limited vibrational motion about a fixed position, whereas at higher temperatures the particles made excursions about other regions of the potential-energy surface. Interestingly, Weissmann and Cohan observed that only the 7- and 19-atom clusters exhibit a clearly defined melting transition region. This observation agrees with the behavior observed for gas-phase clusters; configurations of nonmagic-number-sized clusters exhibit no coexistence of solid and liquid phases, whereas magic number clusters have been found to have definite coexistence regions. For the 7-atom cluster, they observed large fluctuations of several thermodynamic properties in the melting region owing to transitions between solidlike and liquidlike structures. They concluded that accurate thermodynamic averages required a long molecular-dynamics trajectory. The need for long simulation times was a result of incomplete sampling of phase space.

Another molecular-dynamics study[11] of Lennard-Jones clusters adsorbed on a surface focused on the existence of melting transitions in 13-atom clusters as a function of the strength of the adatom–surface interaction. The simulation was intended to study the melting and freezing behavior of an icosahedron adsorbed intact onto a cold surface, described by a model potential having a variety of well depths. Coexistence regions and melting temperatures were observed for a variety of substrate strengths, with the clusters maintaining their three-dimensional structure. On increasing the temperature, intact cluster desorption occurred for the weaker substrate–adsorbate strengths and partial desorption and distortion of the icosahedron occurred for stronger interactions.

The general problem of the incomplete sampling of configuration space (often called quasiergodicity) noticed in the adsorbed cluster problem by Weissmann and Cohan[10] was recently discussed by Frantz, Freeman, and Doll[12] in the study of the melting transition of argon clusters in the vapor phase. Frantz, Freeman, and Doll introduced a method, called J-walking, that greatly reduced the error resulting from quasiergodicity. This method is based on the coupling of the usual Metropolis random walk with another random walk at a higher temperature. Jumps to the higher-temperature distribution are attempted periodically to allow the low-temperature random walk to be transported to a different region of configurational space, hence preventing any confinement of the low-temperature walk only to certain regions of configuration space. As discussed in Sec. IV, the J-walking procedure is used in the current work to avoid quasiergodicity difficulties inherent in the adsorbed cluster problem.

The purpose of the current study is to calculate the thermodynamic quantity ΔG_m^0 for the formation of a cluster of size n by adding one monomer to an $n-1$ cluster for a simulated system of argon particles on a graphite surface. Knowledge of the free energy as a function of cluster size is important, because ΔG_m^0 can enable the calculation of nucleation rates[1,13] as well as provide information about thermodynamic stability. Cluster sizes 2–12 are investigated using Monte Carlo simulations of the argon–graphite system. Problems related to quasiergodicity are presented and solved by implementation of the J-walking method. Similar to the approach taken in Refs. 3 and 4, the existence of minima in the ΔG_m^0 values with respect to size suggest particularly stable clusters.

The contents of the remainder of this paper are as follows. In Sec. II we discuss the theoretical model used in this work. In Sec. III the 0 K lowest classical energy configurations for the different argon clusters adsorbed on a graphite surface are identified with a Brownian dynamics simulated annealing procedure. In Sec. IV the simulation methods and results are presented, and problems related to quasiergodicity are discussed. Relevant details of the Monte Carlo simulation method used in this work are presented, i.e., standard Metropolis simulations and J-walking. The physical implications of our results are also considered in this section. Finally, we summarize our conclusions in Sec. V.

II. THEORETICAL MODEL

There are three interparticle potentials used in this work: the Ar–Ar potential, the Ar–surface potential, and a cluster constraining potential. The representation of the interparticle interactions in terms of pairwise additive potentials is well known. In our work, we have used a simple pairwise Lennard-Jones potential for the description of the interaction between argon atoms. It is well established that satisfactory results for liquid and solid rare gases can be obtained with this level of approximation. Consequently, no effort was made to use a more realistic potential.[14] The form of the Lennard-Jones potential is

$$V_{\mathrm{LJ}}(r)=4\epsilon_{\mathrm{Ar-Ar}}\left[\left(\frac{\sigma_{\mathrm{Ar-Ar}}}{r}\right)^{12}-\left(\frac{\sigma_{\mathrm{Ar-Ar}}}{r}\right)^{6}\right], \tag{1}$$

where, as usual, the quantities $\sigma_{\mathrm{Ar-Ar}}$ and $\epsilon_{\mathrm{Ar-Ar}}$ define the units of length and energy, respectively. In the present study these parameters are $\sigma_{\mathrm{Ar-Ar}} = 3.504$ Å and $\epsilon_{\mathrm{Ar-Ar}} = 119.5$ K.

It has been shown that argon atoms covering a graphite surface form an incommensurate layer;[9] the physisorbed argon atoms arrange themselves in a crystal lattice that is independent of the underlying graphite lattice. The argon film is not in registry with the graphite substrate because the energy of interaction between argon atoms is larger than the lateral variations of their respective interactions with the surface. To a good approximation the graphite can be considered as a perfectly smooth surface that will only act as a template for the adsorbed particles. The interaction potential between Ar and graphite, V_s, is described by the Steele potential[8] previously mentioned. Neglecting corrugation contributions, the form of the potential used here is given by

TABLE I. Argon–graphite potential-energy parameters.

Parameter	Value[a]
A	3.429 Å
q	2
a_s^*	5.241 Å^2
Δz	3.395 Å
$\epsilon_{Ar\text{-}C}$	57.8 K

[a]Reference 8.

$$\frac{V_s(z)}{\epsilon_{Ar\text{-}C}}=\frac{2\pi qA^6}{a_s^*}\left[\frac{2A^6}{5z^{10}}-\frac{1}{z^4}-\frac{1}{3\Delta z(z+0.61\Delta z)^3}\right]. \quad (2)$$

In Eq. (2) z is the perpendicular height of the adatom above the surface in Å; values for the other parameters in the Ar–graphite potential are listed in Table I. The corrugation of the surface does not have to be considered in this work because the contribution to the binding energy of the adsorbed material is small.

As in previous vapor-phase studies,[3] we impose an external constraining potential that acts to define each cluster. The constraining potential V_C used throughout this work for an n-particle cluster is given by

$$V_C=\sum_i^n v_i, \quad (3)$$

where

$$v_i=\begin{cases}0, & |\mathbf{r}_i'|\leq R_C,\\ \infty, & |\mathbf{r}_i'|>R_C.\end{cases} \quad (4)$$

In Eq. (4)

$$\mathbf{r}_i'=\mathbf{r}_i-\mathbf{R}_{cm_{(n-1)}}, \quad (5)$$

where $\mathbf{r}_i$ is the projection of the location of particle i in the plane of the substrate, $\mathbf{R}_{cm_{(n-1)}}$ is the projection of the center of mass of the $n-1$ particle cluster in the plane of the substrate, and R_C is a predetermined constraining radius. The form of this constraining potential is similar to that introduced by Lee, Barker, and Abraham[15] in gas-phase studies. In this work, the constraining potential is taken to enclose a specific area defined by the constraining radius and centered about the center of mass of the $(n-1)$-particle cluster. We choose to center the constraining potential about the $(n-1)$-particle cluster rather than the n-particle cluster because the choice simplifies the calculation of ΔG_m^0 as discussed below. It is not necessary to incorporate a z dependence in the constraining potential because the argon–graphite interaction readily keeps the particles close to the surface at the temperatures considered here. Preliminary calculations have been performed to determine the dependence of the Gibbs free energy on the constraining radius. Values of ΔG_m^0 as a function of R_C have been computed for the Ar_7 cluster. Only a weak dependence on the constraining radii was observed.[16] In all the results reported in this work R_C is taken to be $3\sigma_{Ar\text{-}Ar}$, a radius that is large enough to allow free movement of the particles but small enough to prevent any particles from straying so far from the cluster that they can never recombine during the length of a typical simulation.

The main objective of this study is to calculate the change in Gibbs free energy for the process

$$Ar_{n-1,(a)}+Ar_{(a)}\rightarrow Ar_{n,(a)}, \quad (6)$$

where (a) indicates that the argon particles are adsorbed on a graphite surface and n denotes the number of particles in the cluster. In the approximation that the adsorbed clusters do not interact with each other, the change in the molar Gibbs free energy for this process at temperature T in a standard state of one atmosphere is given by

$$\Delta G_m^0=-RT\ln\frac{q_n^0/L}{(q_{(n-1)}^0/L)(q_1^0/L)}, \quad (7)$$

where L is Avogadro's number, R is the gas constant, and q_n^0 is the molecular partition function for a cluster of size n given by

$$q_n^0=\frac{1}{n!}\frac{1}{h^{3n}}\int d\Gamma\exp[-\beta H(\Gamma)]. \quad (8)$$

In Eq. (8) h is Planck's constant, $\beta=1/k_BT$, k_B is the Boltzmann constant, H is the Hamiltonian, Γ represents the phase-space variables, and the superscript 0 refers to the standard state. Integration of Eq. (8) over all momenta gives

$$q_n^0=\frac{1}{n!}\left(\frac{2\pi mk_BT}{h^2}\right)^{3n/2}\int d^{3n}r\exp[-\beta V(\mathbf{r})], \quad (9)$$

where m is the particle mass and $V(\mathbf{r})$ represents the potential energy of the cluster. The integral on the right-hand side of Eq. (9) is the standard configurational integral, Z_n. By inserting Eq. (9) into (7), the expression for ΔG_m^0 becomes

$$\frac{\Delta G_m^0}{RT}=-\ln\frac{Z_n}{Z_{(n-1)}Z_1}+\ln n-\ln L, \quad (10)$$

where Z_n, $Z_{(n-1)}$, and Z_1 are the configurational integrals for the n-atom cluster, $(n-1)$-atom cluster, and the argon monomer, respectively.

The method we use to evaluate the ratio of configurational integrals is related to the method introduced by Mruzik *et al.*[17] In this method the total cluster potential energy is expressed as a scaled potential of the form

$$V_{tot}=V_{(n-1)}+V_1+\lambda V_{intr}+V_C, \quad (11)$$

where $V_{(n-1)}$ is the total (surface plus cluster) potential energy of the $(n-1)$-particle cluster, V_1 is the interaction potential energy between the surface and the nth monomer, V_{intr} is the interaction between the nth monomer and the other $(n-1)$ particles in the cluster, V_C is the constraining potential, and λ is a scaling factor. Since V_{tot} is a function of λ, the configurational integrals associated with the scaled potential likewise are functions of λ

$$Z_n(\lambda)=\int d^{3n}r\exp[-\beta V_{tot}(\lambda)]. \quad (12)$$

Clearly $Z_n(\lambda=1)=Z_n$ and

$$Z_n(\lambda=0)=\int d^{3n}r \exp[-\beta(V_{(n-1)}+V_1+V_C)]. \tag{13}$$

The above integral can be factored into two separate integrals. The first is $Z_{(n-1)}$, and the second integral I can be expressed as

$$I=\int_{A_C} dx\,dy \exp[-\beta V_{C,1}(x,y)] \int dz \exp[-\beta V_1(z)], \tag{14}$$

where $V_{C,1}(x,y)$ is the interaction of a monomer with the constraining potential. This first integral on the right-hand side of Eq. (14) is just the area A_C contained by the walls of the constraining potential, and we define the second integral factor to be

$$C=\int dz \exp[-\beta V_1(z)], \tag{15}$$

so that

$$I=A_C C. \tag{16}$$

The configurational integral of the monomer, Z_1, is given by

$$Z_1=\int d^3r \exp[-\beta V_1(z)] \tag{17}$$

$$=A\int \exp[-\beta V_1(z)]dz=AC, \tag{18}$$

where A is the area of surface occupied by one mole of monomers. The values for this area can be obtained as a function of temperature using the ideal-gas law. At equilibrium the chemical potentials of the vapor and adsorbed phases are equal. By equating the chemical potentials and invoking the ideal-gas law, one obtains the following expression for the molar area occupied by the surface species as a function of the external pressure p:

$$A=RT/pC. \tag{19}$$

The evaluation of C [Eq. (15)] has been discussed elsewhere[9] and in the current application approximately equals 0.130 Å.

From Eqs. (14) and (18), we obtain

$$Z(\lambda=0)=Z_{(n-1)}Z_1\frac{A_C}{A}, \tag{20}$$

so that

$$\ln\frac{Z_n}{Z_{(n-1)}Z_1}=\ln\frac{Z(\lambda=1)}{Z(\lambda=0)}+\ln\frac{A_C}{A}. \tag{21}$$

We also can write

$$\ln\frac{Z(\lambda=1)}{Z(\lambda=0)}=\int_0^1 \frac{d\ln Z}{d\lambda}d\lambda \tag{22}$$

and

$$-\frac{1}{\beta}\frac{d\ln Z}{d\lambda}=\frac{\int V_{\rm intr} d^{3n}r \exp(-\beta V_{\rm tot})}{\int d^{3n}r \exp(-\beta V_{\rm tot})}=\langle V_{\rm intr}\rangle_\lambda. \tag{23}$$

Using Eqs. (22) and (23) and substituting in Eq. (10), the following expression is obtained for ΔG_m^0:

$$\frac{\Delta G_m^0}{RT}=\beta\int_0^1 \langle V_{\rm intr}\rangle_\lambda d\lambda+\ln\frac{A}{A_C}+\ln n-\ln L. \tag{24}$$

Equation (23) can be evaluated by the standard Metropolis Monte Carlo procedure.[18] As will be discussed in Sec. IV, the evaluation of $\langle V_{\rm intr}\rangle_\lambda$ as a function of λ presented sampling problems similar to those observed for argon clusters in the gas phases near the melting transition region.

III. SIMULATED ANNEALING STUDIES

To obtain the minimum-energy configurations of argon clusters on a graphite surface a simulated annealing study, similar to the one used by Zhang, Freeman, and Doll in a study of HF clusters,[4] was used. The simulated annealing approach used in this work propagates the motion of the particles according to the Langevin equation,

$$\frac{d\mathbf{v}_i}{dt}=-\gamma\mathbf{v}_i+(1/m_i)\mathbf{F}_1+(1/m_i)\mathbf{F}_2, \tag{25}$$

where γ is a friction constant, $\mathbf{v}_i$ is the velocity of particle i, m_i is the mass of particle i, $\mathbf{F}_1$ is the force on the particle i from the other particles, the constraining potential, and the graphite surface, and $\mathbf{F}_2$ is a random force. The properties of $\mathbf{F}_2$ and the method used to solve Eq. (25) are given in Chandrasekhar's review of Brownian motion.[19]

For each cluster size, Eq. (25) was solved at an initial temperature of 300 K for a warm-up period, followed by an instantaneous cooling to 0 K. During the cooling process the particles assumed a configuration consistent with one of their near-local minima. Since there can be many local minima in the potential-energy surface, there was no guarantee that the absolute minimum-energy configuration was obtained. Furthermore, the number of local minima in the potential-energy function increases with cluster size. To increase confidence that the absolute minimum was located, from 100 to 1300 trajectories were calculated for each cluster size.

At the energy minimum the dimers have an internuclear separation of $r_0=2^{1/6}\sigma_{\rm Ar-Ar}$ at a distance $z_{\rm min}$ above the surface, where $z_{\rm min}$ is the equilibrium distance at which a monomer resides above the model substrate (3.408 Å). The three particle clusters form an equilateral triangle, each particle also r_0 apart, and with the triangle in a plane parallel to the graphite surface at a height $z_{\rm min}$. Figure 1 illustrates the 0 K minimum-energy configuration for the 12-atom cluster. The minimum-energy structure for other clusters can be obtained from this figure by removing the extra atoms; e.g., Ar_4 consists of those atoms labeled 1–4, Ar_6 consists of those atoms labeled 1–6, and so on. Consistent with the findings of Weissmann and Cohan,[10] the minimum-energy Ar_6 cluster is a centered hexagon with the particle that would complete the ring missing. The minimum-energy structure for Ar_7 is a centered hexagon,

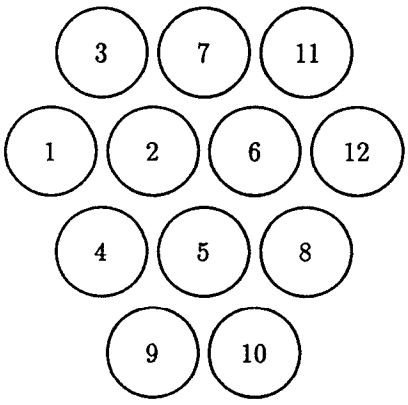

FIG. 1. Zero kelvin minimum-energy configuration for Ar_{12} adsorbed on a graphite substrate. The minimum-energy configurations for clusters of size n where $n < 12$ are obtained by including only those atoms numbered 1 through n.

also consistent with Weissmann and Cohan. The nearest-neighbor bond lengths in the hexagon are all within about 1% of r_0.

It is of interest to compare the growth sequence obtained in the current study for argon clusters adsorbed on graphite with that observed in previous gas-phase studies.[20,3] The minimum-energy structures for gas-phase Lennard-Jones clusters, at least for cluster sizes 7–19, increase in size via an icosahedral growth scheme. A detailed discussion of this set of clusters is given in Ref. 3. In the vapor phase, addition of an atom to a cluster of size 7 to form a cluster of size 8 results in an increased total binding energy of approximately $3\epsilon_{Ar-Ar}$. This same increase in total binding energy is found in increasing the cluster size by monomer addition until the addition of one atom to an 11-particle cluster to form the 12-particle cluster. In this case, the increase in binding energy is approximately $4\epsilon_{Ar-Ar}$. With the addition of a monomer to the 12-particle cluster to form a 13-particle cluster, a shell is closed to form a complete icosahedron with a gain in binding energy of approximately $6\epsilon_{Ar-Ar}$. The large increase in the number of nearest-neighbor bonds resulting from shell closings is the principal cause of the extra thermodynamic stability of the magic-number-sized clusters. For the case of adsorbed argon atoms on the model graphite substrate, the growth scheme is hexagonal, and each addition of an atom for cluster sizes from 2 through 6 increases the cluster contribution to the total binding energy by approximately $2\epsilon_{Ar-Ar}$. With the completion of the hexagon to form a cluster of size 7, the increase in the cluster contribution to the total binding energy is approximately $3\epsilon_{Ar-Ar}$. For adsorbed clusters of argon atoms, we can expect magic numbers at cluster sizes 7, 10, and 12. The increase in the cluster contribution to the total binding energy for adsorbed clusters is less than the increase for vapor-phase clusters, and more shallow minima in the thermodynamic properties associated with magic number behavior can be expected.

While the configurations obtained here are the lowest-energy arrangements only for the laterally averaged surface interaction case, the experimental evidence that argon forms an incommensurate layer[21] suggests that the configurations would not change on addition of the corrugation term to the potential used here.[8,9] The height of the particles above the surface would change, however, since the energy of interaction with the surface does change as the adatom moves over the surface. It might be expected that quenches incorporating a corrugation term would result in configurations whose projected two-dimensional structure are the same as those observed here, but no longer lie in the same plane above the surface.

In addition to the minimum-energy structures, many high-energy isomer structures were obtained from the simulated annealing trajectories. Like the energy minima, the high-energy isomers found during the quenches lie in the z_{min} plane and no three-dimensional structures were encountered. When the four-particle cluster was initialized as a tetrahedron on the surface at 0 K, it was found to be a local minimum of the potential surface. However, the high energy found for the tetrahedral structure implied it to be of minimal physical significance in the argon–graphite system. As expected, the number of isomers increased dramatically with cluster size. The energy differences between the isomers, particularly for the larger clusters, were small. For example, 17 isomers were found for the 9-particle cluster with a difference in energy between the highest and lowest isomers of only $1.28\epsilon_{Ar-Ar}$, or about 1.5% of the total energy of the lowest-energy configuration.[16]

IV. SIMULATION METHODS AND RESULTS

The Gibbs free energies for the growth of argon clusters on graphite were calculated from Eqs. (23) and (24). Initially, the potential energies of the adsorbed clusters were computed using standard Monte Carlo methods. To begin the simulations, each argon cluster was placed in its lowest-energy configuration at 0 K. The particles were then moved using a Metropolis box size such that 50% of the moves were accepted. The length of the warm-up period for all values reported here was one million moves. Averages were taken over 10 subsequent blocks of 100 000 moves. The reported Monte Carlo results are averages over the 10 block means. The λ integration in Eq. (23) was performed numerically using Gauss–Legendre quadrature. Preliminary calculations were performed to obtain the dependence of the integrated interaction energy $(\int_0^1 \langle V_{intr} \rangle_\lambda d\lambda)$ on the number of Gauss points included. The values for the integrated interaction energy for Ar_7 obtained using 4–12 quadrature points all lie within a standard deviation of each other. For reasonable computational efficiency, the results reported below were determined with 6 Gauss–Legendre points.

As mentioned previously, we encountered sampling difficulties in performing the Monte Carlo integrations. The origin and nature of these sampling difficulties can be understood by examining Fig. 1 and focusing on the four-particle cluster (i.e., consider only atoms numbered 1–4). From Fig. 1 it can be seen that the argon–argon interaction energies will have two different magnitudes. The largest

interaction energy comes from the nearest-neighbor bonds, as for example between atoms numbered 1 and 2. In addition, there is a weaker interaction between the atoms numbered 3 and 4. At finite temperatures the four-particle cluster undergoes oscillations to structures where atoms 3 and 4 become near neighbors and atoms 1 and 2 become farther apart. Since such a structure has the identical energy to the original structure, no energy fluctuations can be anticipated from such oscillatory motions in the calculation of the internal energy. However, the Gibbs free energy is calculated using the scaled potential [Eq. (11)]. When the scaled potential is used, one of the four atoms in the cluster has a different interaction with the remainder of the cluster than the other three. The oscillatory motion has the possibility of introducing significant fluctuations in the Monte Carlo evaluation of $\langle V_{\text{intr}}\rangle_\lambda$. Such serious fluctuations were found in the Metropolis walks for the tetramer when λ exceeded 0.8. We were able to confirm[16] the origin of the fluctuations by monitoring the bond lengths in the cluster and correlating the bond-length fluctuations with fluctuations in the calculated values of V_{intr}. The quasiergodicity problems were sufficiently severe that satisfactory results were impossible to obtain by using Metropolis sampling with walks of reasonable length.

To solve the quasiergodicity difficulties in the Monte Carlo simulations, we used the J-walking method.[12] As stated previously, this approach is based on coupling the usual Metropolis random walk with periodic jumps to another random walker at a higher temperature. In the standard Metropolis algorithm, a random walker samples configuration space from an initial position x_i to a final position x_f with a probability of acceptance

$$p=\min[1,q(x_f|x_i)], \tag{26}$$

where

$$q(x_f|x_i)=\frac{T(x_i|x_f)\rho(x_f)}{T(x_f|x_i)\rho(x_i)}, \tag{27}$$

$\rho(x)$ is the Boltzmann distribution and $T(x'|x)$ the sampling distribution that is usually generated from uniform deviates over a finite range.[22] In the J-walking technique the sampling distribution for the jumps is the Boltzmann distribution at a higher temperature β_J

$$T_J(x'|x)=Z^{-1}\exp[-\beta_J V(x')]. \tag{28}$$

With use of Eq. (28), $q(x'|x)$ becomes

$$q(x'|x)=\exp\{(\beta_J-\beta)[V(x')-V(x)]\}. \tag{29}$$

In applying J-walking to the argon–graphite system, the high-temperature distribution was generated and saved in an external array for subsequent sampling by the low-temperature walker. Specifically, a distribution at a higher temperature (20 K in all cases) was generated starting from the 0 K equilibrium structure. This 20 K distribution was generated from one long Metropolis walk consisting of 10^6 warm-up moves and 5×10^6 moves, where a configuration was stored every 100 moves. Calculations at 20 K showed that distributions generated under these conditions were ergodic. The results at 10 K were obtained by jumping to the 20 K distribution every 10 passes.

TABLE II. Integrated interaction energies and Gibbs free energies at 10 K.[a]

n	$\int_0^1\langle V_{\text{intr}}\rangle_\lambda d\lambda$	$\int_0^1\langle V_{\text{intr}}\rangle_\lambda^{j-w}d\lambda$	ΔG_m^0	ΔG_m^{0j-w}
3	-1.452 ± 0.003	-1.448 ± 0.002	-1.069 ± 0.003	-1.066 ± 0.002
4	-1.65 ± 0.08	-1.647 ± 0.001	-1.24 ± 0.08	-1.241 ± 0.001
7	-2.50 ± 0.04	-2.483 ± 0.004	-2.05 ± 0.04	-2.036 ± 0.004
12	-2.65 ± 0.07	-2.640 ± 0.004	-2.15 ± 0.07	-2.142 ± 0.004

[a]$\langle V_{\text{intr}}\rangle^{j-w}$ and ΔG_m^{0j-w} are values obtained using J-walk Monte Carlo simulations. The results are expressed in units of $\epsilon_{\text{Ar-Ar}}$.

Gibbs free energies and integrated interaction energies at 10 K are given in Table II for clusters Ar_3, Ar_4, Ar_7, and Ar_{12} using both standard Metropolis and J-walking techniques. All values are averages over one million passes and are reported with single standard-deviation error bars. It can be seen from this table that for cluster sizes $n=4$, $n=7$, and $n=12$ the J-walking decreases the standard deviation by at least a factor of 10, hence diminishing the sampling problem previously mentioned. Additionally, results for $n=4$ clusters using J-walking show the expected $1/\sqrt{(N)}$ behavior of the standard deviation suggesting the walks were ergodic. Table III shows the Gibbs free energies and integrated interaction energies at 10 K for all clusters considered here using J-walking. The sampling problems observed for clusters $n=4$, 5, and 6 were eliminated using the J-walking technique.

Figure 2 shows a graph of ΔG_m^0 as a function of cluster size. There are three different minima in the Gibbs free energy at $n=7$, 10, and 12. These three cluster sizes are those expected to be most stable from the discussion presented in Sec. III concerning Fig. 1. The small differences in stability for the $n=4$, 5, and 6 clusters arise from other than nearest-neighbor interactions. Figure 3 presents a graph of ΔU_m^0 as a function of cluster size. ΔU_m^0 reflects the same magic number behavior observed for ΔG_m^0.

TABLE III. Integrated interaction energies and Gibbs free energies at 10 K.[a]

n	$\int_0^1\langle V_{\text{intr}}\rangle_\lambda d\lambda$	ΔG_m^0
2	-0.693 ± 0.001	-0.345 ± 0.001
3	-1.448 ± 0.002	-1.066 ± 0.002
4	-1.647 ± 0.001	-1.241 ± 0.001
5	-1.743 ± 0.002	-1.318 ± 0.002
6	-1.834 ± 0.002	-1.394 ± 0.002
7	-2.483 ± 0.004	-2.036 ± 0.004
8	-1.800 ± 0.002	-1.336 ± 0.002
9	-1.865 ± 0.003	-1.391 ± 0.003
10	-2.597 ± 0.004	-2.114 ± 0.004
11	-1.901 ± 0.004	-1.410 ± 0.004
12	-2.640 ± 0.004	-2.142 ± 0.004

[a]All quantities are expressed in units of $\epsilon_{\text{Ar-Ar}}$. All values were calculated using J-walking.

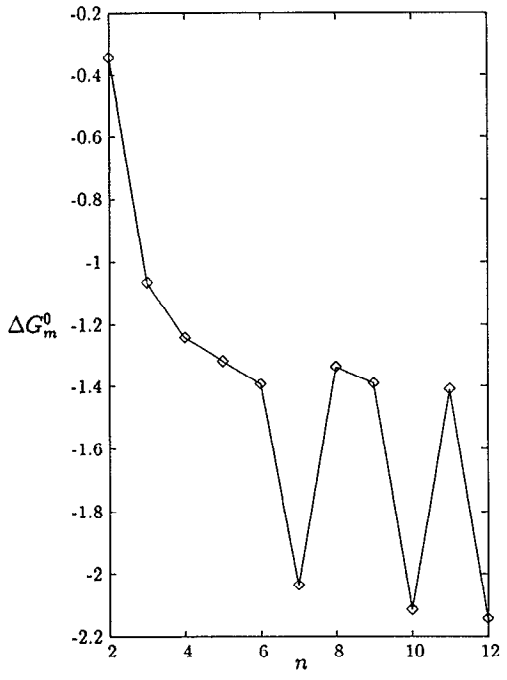

FIG. 2. ΔG_n^0 as a function of n at 10 K. The free energy is expressed in units of $\epsilon_{Ar\text{-}Ar}$. The points are connected by straight lines for clarity.

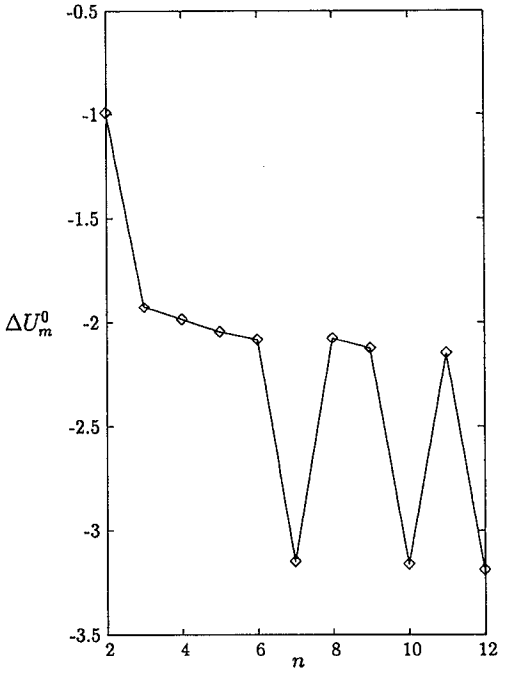

FIG. 3. ΔU_n^0 as a function of n at 10 K. The internal energy is expressed in units of $\epsilon_{Ar\text{-}Ar}$. The points are connected by straight lines for clarity.

V. CONCLUSIONS

As found in previous studies of the properties of clusters in the vapor phase, we see a strong correlation between the structure of adsorbed clusters and their associated thermodynamic properties. The existence of the local minima in the Gibbs free energy of the clusters as a function of cluster size is driven by energetics. The locations of the magic numbered minima are explained by a simple bond counting model, analogous to the models used in gas-phase studies.

The sampling difficulties encountered in determining the Gibbs free-energy changes for adsorbed clusters are significantly worse than for simulations of single-component clusters in the vapor phase. In the vapor phase, the sampling problems are an issue at melting temperatures where the single-component clusters begin to access their high-energy isomers. For the adsorbed clusters sampling difficulties occur at low temperatures because the adsorbed aggregates have significant numbers of low-energy "breathing" modes not present in the three-dimensional structures. These sampling problems were particularly problematic for the small clusters and readily solved with the J-walking method.

The sampling difficulties discussed in the preceding paragraph suggest an avenue to the calculation of free-energy differences between isomers of the same cluster size. Consider the lowest-energy isomer for a cluster of size seven (atoms 1–7 in Fig. 1). A higher-energy 7-atom cluster can be formed in Fig. 1 by including atoms 1–6 and atom number 8, but excluding atom number 7. In calculating the free energy for the growth of a 7-atom cluster to an 8-atom cluster, we have the choice of scaling the interaction of either atom number 7 or 8 by λ. In the calculations reported in this work, we chose to scale atom 8, because this choice is associated with the process of adding an atom to the lowest-energy 7-atom cluster. If we had scaled atom number 7 instead, the free-energy change would be that associated with forming the lowest-energy 8-atom cluster from a high-energy 7-atom cluster. The difference between the free energies calculated by scaling different atoms can be expected to be the free-energy difference between the two 7-atom clusters (the final state is the same in each case). There are several sampling issues connected with this approach, and the utility of the method is under current investigation.

ACKNOWLEDGMENTS

We would like to thank Professor Don Frantz, Professor Jan Northby, and Professor Jim Doll for helpful discussions. Acknowledgment is made to the Donors of the Petroleum Research Fund of the American Chemical Society for support of this work.

[1] F. F. Abraham, *Homogeneous Nucleation Theory* (Academic, New York, 1974).
[2] R. H. Berry, T. L. Beck, and H. L. Davis, in *Advances in Chemical Physics*, edited by I. Prigogine and S. A. Rice (Wiley, New York, 1988), Vol. 70B, p. 75.
[3] D. L. Freeman and J. D. Doll, in *Advances in Chemical Physics*, edited by I. Prigogine and S. A. Rice (Wiley, New York, 1988), Vol. 70B, p. 139.
[4] C. Zhang, D. L. Freeman, and J. D. Doll, J. Chem. Phys. **91**, 2489 (1989).
[5] O. Echt, K. Sattler, and E. Recknagel, Phys. Rev. Lett. **47**, 1121 (1981).

[6] I. A. Harris, R. S. Kidwell, and J. A. Northby, Phys. Rev. Lett. **53**, 2390 (1984).
[7] Some examples are A. Cheng and W. A. Steele, Langmuir **5**, 600 (1989); M. J. Bojan and W. A. Steele, *ibid.* **5**, 625 (1989); V. Bhethanabotla and W. A. Steele, J. Phys. Chem. **92**, 3285 (1988); M. L. Klein, S. O'Shea, and Y. Ozaki, *ibid.* **88**, 1420 (1984); C. G. Shaw, S. C. Fain, and M. D. Chinn, Phys. Rev. Lett. **41**, 955 (1977).
[8] W. A. Steele, Surf. Sci. **36**, 317 (1973).
[9] W. A. Steele, *Interactions of Gases with Solid Surfaces* (Pergamon, Oxford, 1974).
[10] M. Weissmann and N. V. Cohan, J. Chem. Phys. **72**, 4562 (1980).
[11] E. Blaisten-Barojas, I. L. Garzon, and M. Avalos-Borja, Phys. Rev. B **36**, 8447 (1987).
[12] D. D. Frantz, D. L. Freeman, and J. D. Doll, J. Chem. Phys. **93**, 2769 (1990).
[13] B. Lewis and J. C. Anderson, *Nucleation and Growth of Thin Films* (Academic, New York, 1978).
[14] R. A. Aziz, in *Inert Gases*, edited by M. L. Klein (Springer-Verlag, Berlin, 1984), p. 5.
[15] J. K. Lee, J. A. Barker, and F. F. Abraham, J. Chem. Phys. **58**, 3166 (1973).
[16] M-A. Strozak, M. S. thesis, University of Rhode Island, 1991 (unpublished).
[17] M. R. Mruzik, F. F. Abraham, D. E. Schreiber, and G. M. Pound, J. Chem. Phys. **64**, 481 (1976).
[18] N. Metropolis, A. W. Rosenbluth, M. N. Rosenbluth, A. H. Teller, and E. Teller, J. Chem. Phys. **21**, 1087 (1953).
[19] S. Chandrasekhar, Rev. Mod. Phys. **15**, 1 (1943).
[20] M. R. Hoare and P. Pal, Adv. Phys. **20**, 161 (1971).
[21] F. F. Abraham, in *Molecular-Dynamics Simulation of Statistical-Mechanical Systems*, edited by G. Ciccoti and W. G. Hoover (North-Holland, Amsterdam, 1986), Pt. II, p. 130.
[22] M. H. Kalos and P. A. Whitlock, *Monte Carlo Methods* (Wiley, New York, 1986).